Sensorless vector control of Dual Star induction Motor Associated with Fuzzy Mutual–MRAS estimator in electric vehicle

Ismail BENMILOUD, Katia KOUZI, Aissa AMEUR

Laboratory of Semiconductors and Functional Materials, Amar Telidji University of Laghouat, Algeria

is.benmiloud@lagh-univ.dz, k.kouzi@lagh-univ.dz, a.ameur@lagh-univ.dz

Abstract: Sensorless control has become an attractive and important topic from an industrial perspective. The presence of sensors in electronic speed drives can reduce their robustness and reliability while increasing costs and mounting complexity. Therefore, mechanical sensors will be replaced by a calculation algorithm that provides speed estimation from the electrical terminal of the machine. It is imperative that the performance required from this estimator be close to or similar to that provided by a physical sensor. In this paper, different estimation and observation techniques will be presented. Then, Sensorless vector control based on a mutual - MRAS estimator and Fuzzy mutual - MRAS estimator for Dual Star induction Motor (DSIM) to estimate the speed, as well as the resistances for both the stator and rotor will be introduced. Finally, the results of the simulation will be shown and discussed.

Keywords: Dual Star Induction Motor, Sensorless vector control, Fuzzy mutual-MRAS estimator, electric vehicle.

1. Introduction

The use of dual-star induction motor drives in electric vehicles provides several benefits compared to DC machines, such as reliability, smaller size, absence of brushes, lower cost and reduced maintenance (Bhatt, Mehar & Sahajwani, 2019), (Pellegrino et al., 2011), (Hashemnia & Asaei, 2008). However, conventional field-oriented control of an induction motor (IM) requires a speed sensor to function properly. The use of this sensor necessitates additional electronic devices, more space, increased wiring and precise installation, thereby reducing the reliability of the controller system (Holmes, McGrath & Parker, 2011), (Jain et al., 2020), (Chakraborty & Hori, 2003). Moreover, at low power, the cost of the sensor is approximately the same as that of the motor. To overcome these problems, many studies have focused on research techniques that eliminate the need for speed sensors while maintaining a high level of performance. These techniques, known as sensorless techniques (Verma et al., 2013), (Guzinski & Abu-Rub, 2013), (Casadei et al., 2003), present both technical and financial challenges. However, they offer several advantages, including lower cost, reduced maintenance requirements, reduced measurement noise, elimination of the sensor cable, and improved reliability.

2. Field-oriented control for DSIM

To achieve high torque and speed performance in an induction motor (IM) drive, the field-oriented control strategy proves to be highly efficient. The concept behind this technique is to emulate the behaviour of separately excited DC motor drives using the Dual Star induction Motor, which inherently exhibits decoupling between electromagnetic torque and magnetic flux. The state equation of the proposed motor in the dq reference frame is utilized to eliminate the quadrature component of the flux (Andriamalala, Razik & Sargos, 2008), (Sadouni & Meroufel, 2012), (Merabet et al., 2007) by expressing that:

$$\begin{cases} \varphi_{dr} = \varphi_r^* \\ \varphi_{dr} = 0 \end{cases} \tag{1}$$

It is obtained:

$$w_{gl}^* = \frac{R_r . L_m}{(L_m + L_r)} . \frac{(i_{qs1} + i_{qs2})}{\varphi_r^*} \tag{2}$$

$$T_{em}^* = p . \frac{L_m}{(L_m + L_r)} . \varphi_r^* (i_{qs1} + i_{qs2}) \tag{3}$$

To achieve robust control, it is important to know of the value w_{gl}^* however, consistently obtaining this value can be challenging as it is dependent on the resistance, which can vary due to temperature fluctuations. In the next section, a technique to estimate the motor resistance is presented.

3. Sensorless speed control

Modern industrial applications that utilize asynchronous variable speed drives, particularly electric vehicles demanding high dynamic and static performance, rely on orientation and/or flux control techniques (Montanari et al., 2007). These techniques necessitate accurate knowledge of the position, flux modulus, and/or motor speed. This information is typically obtained through feedback control using direct electrical sensors (such as currents, voltages, and flux) or mechanical sensors (such as rotational speed and angular position). However, these sensors sometimes require specialized signal processing for the received physical signals.

Furthermore, the elimination of the mechanical speed sensor can bring economic benefits and enhance operational reliability. Additionally, control without a speed sensor must deliver performance that is comparable to that of a physical sensor, with minimal deviation.

3.1. Speed estimation using MRAS technique

This technique is based on an adaptive system that utilizes an MRAS (Model Reference Adaptive System) model (El Ouanjli et al., 2022), which consists of two flux estimators as illustrated in Figure 1. One of these estimators, known as the reference model (voltage model), does not include speed. The other estimator is the adjustable model (current model), which takes into account the speed. The error resulting from the disparity between the outputs of the two estimators (flux, emf, reactive power), along with the estimated speed generated by an adaptation algorithm, is addressed in previous studies (Singh, Kachhwaha & Fulwani, 2022), (Cardenas et al., 2005).

Nevertheless, the speed estimate-based MRAS technique has a significant drawback, which is its high sensitivity to machine parameters. To address this issue, several studies have proposed online adaptation techniques utilizing either the stator resistance or the rotor resistance. However, the current model is also sensitive to the rotor time constant, and adapting it simultaneously with speed estimation poses challenges (Yang & Chin, 1993) (Mitronikas, Safacas & Tatakis, 2001).
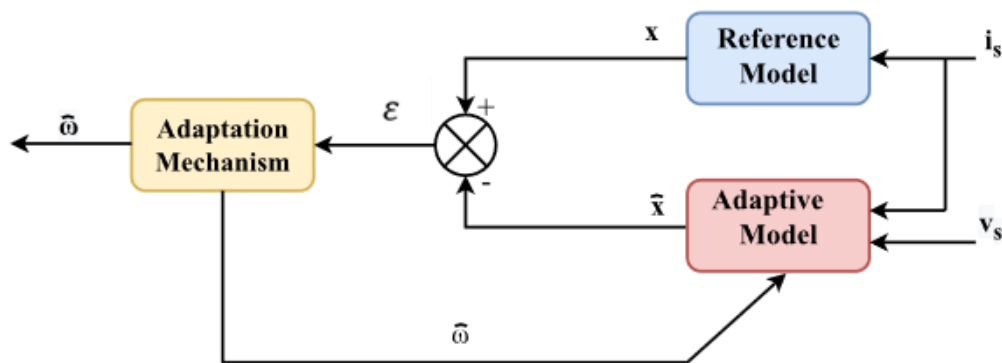
Figure 1. MRAS Structure

3.2. Speed estimation using mutual-MRAS technique

In the mutual MRAS approach, two rotor flux estimators are compared. This approach enables the estimation of both the rotational speed and stator resistance of the DSIM. Figure 2 illustrates the structure of the Mutual MRAS, which consists of a reference model (voltage model), an adjustable model (current model), and two adaptation mechanisms.

3.2.1. Reference model

Regarding the voltage model, the stator equation is described as a reference model in the stationary reference frame (α, β). It generates the reference value for the rotor flux component (Sahraoui, Ameur & Kouzi, 2018). The following equations represent the two reference rotor flux components determined from the reference model:

$$\frac{d\varphi_{r\alpha v}}{dt} = \frac{L_r + L_m}{L_m}\left[v_{s\alpha 1} - r_s \cdot i_{s\alpha 1} - \sigma\left(L_s + L_m\right)\cdot\frac{di_{s\alpha 1}}{dt} - \frac{L_r \cdot L_m}{L_m + L_r}\cdot\frac{di_{s\alpha 2}}{dt}\right] \tag{4}$$

$$\frac{d\varphi_{r\beta v}}{dt} = \frac{L_r + L_m}{L_m}\left[v_{s\beta 1} - r_s \cdot i_{s\beta 1} - \sigma\left(L_s + L_m\right)\cdot\frac{di_{s\beta 1}}{dt} - \frac{L_r \cdot L_m}{L_m + L_r}\cdot\frac{di_{s\beta 2}}{dt}\right] \tag{5}$$

3.2.2. Adaptive model

The current model utilizes the speed value and current input signals to compute the rotor flux components. This model describes the DSIM rotor voltage equation in the stator reference frame (Sahraoui, Kouzi & Ameur, 2017) as follows:

$$\frac{d\varphi_{r\alpha i}}{dt} = \frac{L_m}{T_r}\left(i_{s\alpha 1} + i_{s\alpha 2}\right) - \frac{1}{T_r}\cdot\varphi_{r\alpha i} - \omega_r \cdot \varphi_{r\beta i} \tag{6}$$

$$\frac{d\varphi_{r\beta i}}{dt} = \frac{L_m}{T_r}\left(i_{s\beta 1} + i_{s\beta 2}\right) - \frac{1}{T_r}\cdot\varphi_{r\beta i} - \omega_r \cdot \varphi_{r\alpha i} \tag{7}$$

3.2.3. Adaptation mechanism

Two adaptation mechanisms take the error signals $e_{\varphi r}$ and e_{Rs} as input, with significant differences between the two flux estimators (Touam et al., 2021).

$$e_{\varphi r} = \varphi_{r\beta v}\cdot\varphi_{r\alpha i} - \varphi_{r\alpha v}\cdot\varphi_{r\beta i} \tag{8}$$

$$e_{Rs} = i_{s\alpha}\left(\varphi_{r\alpha v} - \varphi_{r\alpha i}\right) + i_{s\beta}\left(\varphi_{r\beta v} - \varphi_{r\beta i}\right) \tag{9}$$

To minimize errors $e_{\varphi r}$ and e_{Rs}, the adaptation mechanisms deliver both estimated speed and stator resistance by reinjecting them into their respective adjustable models.

The adaption rule, as described (Rsn et al., 2016) can be expressed as follows:

$$\omega_r = k_{p\omega r}\cdot e_{\varphi r} + k_{i\omega r}\cdot\int e_{\varphi r}\cdot dt \tag{10}$$

$$R_s = k_{pRs}\cdot e_{Rs} + k_{iRs}\cdot\int e_{Rs}\cdot dt \tag{11}$$

Where: $k_{p\omega r}$, $k_{i\omega r}$, and k_{pRs}, k_{iRs}: are respectively the gains of the two PI controllers.
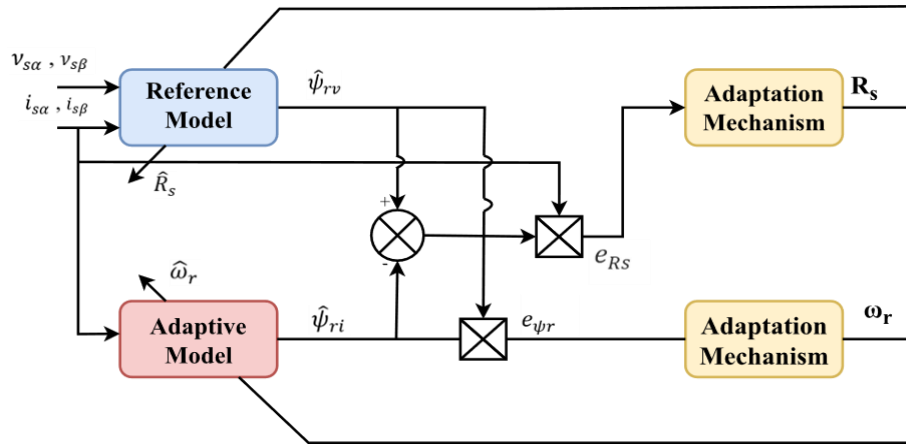
Figure 2. The suggested mutual-MRAS estimator structure

The rotor resistance can then be determined by the following relation:

$$R_r = R_r \cdot \frac{R_{rn}}{R_{ns}}$$

(12)

3.3. Speed estimation using fuzzy mutual-MRAS Technique

The performance of the suggested fuzzy mutual-MRAS estimator is presented. The Figure 3 illustrates the structure of the proposed estimator as described by (Rsn et al., 2016).
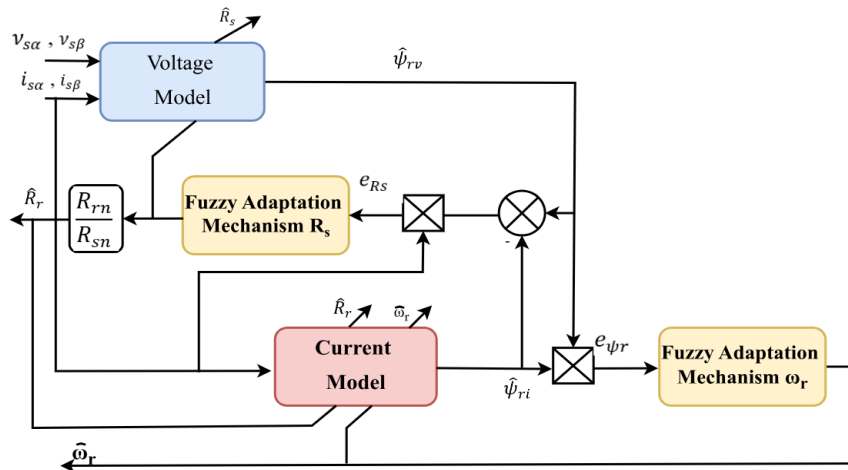
Figure 3. Structure of fuzzy Mutual MRAS estimator

The concept of this approach involves modifying the estimator structure by replacing the traditional PI regulators and adaptation mechanisms with intelligent PI fuzzy controllers (Touam et al., 2021). This modification aims to enhance the performance of the estimator.

4. Vehicle dynamics

When considering the dynamics of the vehicle, it is observed that the tractive force needs to overcome various resistive forces, including grading resistance (Fg), aerodynamic drag (Fw), rolling resistance (F_r), and inertial effects (F_i) (Ehsani et al., 2008). These forces can be represented by the following equation and are illustrated in Figure 4:

$$F_{tractive} = F_w + F_i + F_g + F_r$$

(13)

Aerodynamic drag can be characterized by air density ρ, vehicle body form, vehicle frontal area A_f, and vehicle speed V (Lian et al., 2016).

$$F_w = \frac{1}{2} \rho . A_f . C_D \left(V - V_W \right)^2$$
(14)

Where V_W, V is a measure of the wind speed and C_D is the aerodynamic drag coefficient that describes the form of the vehicle body.

Acceleration Force represents the dynamic of the vehicle in terms of acceleration or braking (Ehsani et al, 2008). It can be calculated using the following equation:

$$F_{acc} = M \frac{dV}{dt} = M . \gamma$$
(15)

γ: vehicle acceleration.

As a result of the elastic material of the tire, a resistance force against rotational movement is produced in front of the wheel center. The following equation is used to calculate the tire rolling resistance:

$$F_r = M . g . C_r$$
(16)

Where: M and C_r represent the vehicle mass, rolling resistance coefficient.

If a vehicle moves on a sloping road, gravity creates a resistive force (Husain, and Islam, 1999). which can be represented by the gradient of path degree α as follows:

$$F_g = M . g . \sin(\alpha)$$
(17)
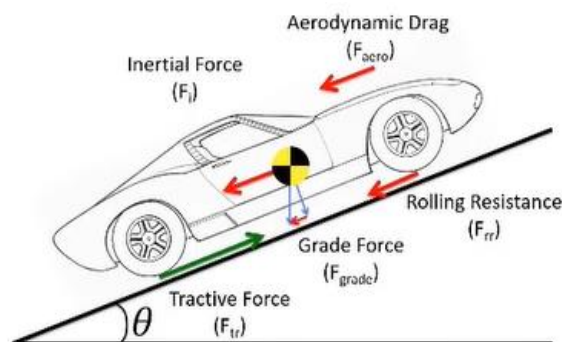
Figure 4. Representation of dynamic vehicles

Where Table 1 and Table 2 represent the studied EV used in simulation, and motor parameters respectively.

Table 1. Main vehicular parameters

Name	Value	Unit
vehicle mass	820	kg
Vehicle frontal area	2.7	m2
Aerodynamic drag coefficient	0.25	-
Air density	1.23	kg.m-3
Wheel radius	0.3	m
Gravity	9.81	m/s2
rolling resistance coefficient	0.01	-

Table 2. Parameters of dual star motor used in the simulation

Nominal Voltage (*V*):	$Vn = 220/380$
Nominal Current (*A*):	$In = 6.5$
Nominal Speed (*rd/s*):	314
Stator Resistance (Ω):	$RS1 = RS2 = 3.72$
Rotor Resistance (Ω):	$Rr = 2.12$
Stator Inductance (*H*):	$LS1 = LS2 = 0.022$
Rotor Inductance (*H*):	$Lr = 0.006$
Mutual Inductance (*H*):	$Lm = 0.3672$
Moment of Inertia (*Kg.m2*):	$J = 0.0625$
Coefficient of Friction (*Nms/rd*):	$Kf = 0.001$
Nominal Frequency (*Hz*):	$f = 50$
Number of Pairs Poles:	$P = 1$

5. Simulation results

To evaluate the performance and stability of the proposed Fuzzy Mutual-MRAS estimator, several tests were conducted under various dynamic operating conditions. These tests included scenarios with abrupt changes in command speed. The purpose of these tests was to assess the effectiveness of the estimator and ensure the stability of the overall system.
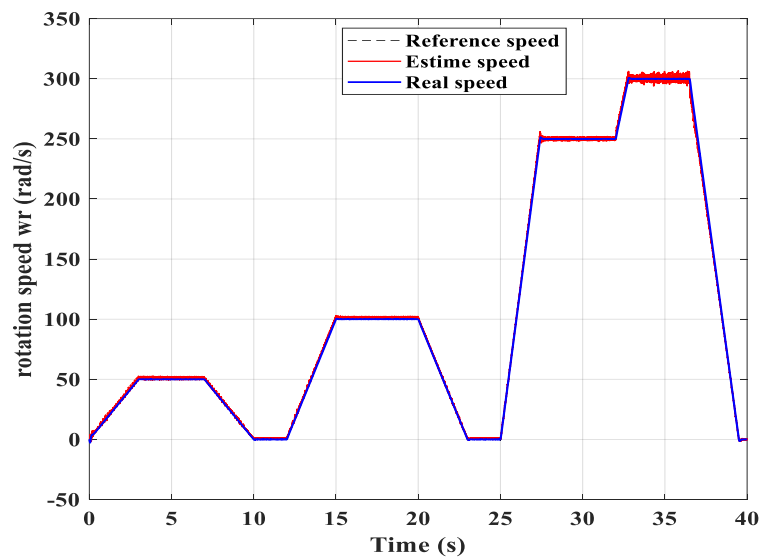
Figure 5. The rotation speed motor
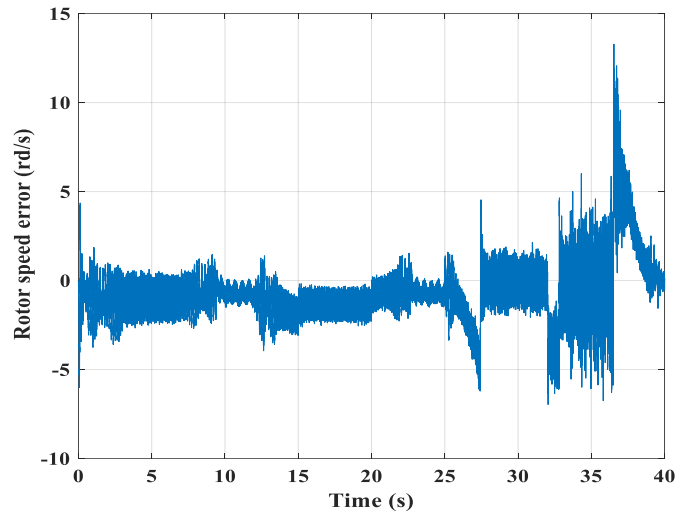
Figure 6. The rotor error speed estimation
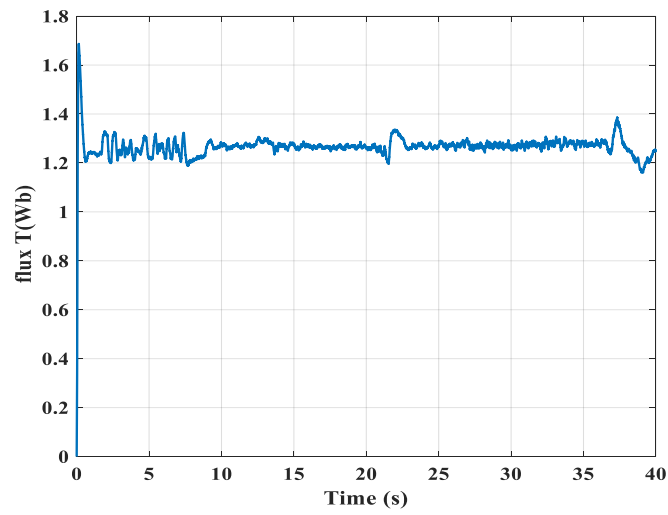
Figure 7. The total flux
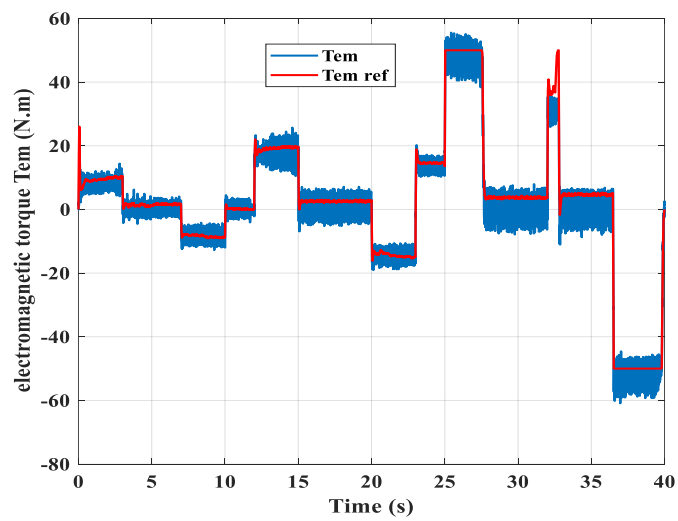
Figure 8. The motor electromagnetic torque

The estimated speed demonstrates rapid convergence, indicating the capability to maintain accurate estimation across different speed levels with an acceptable error. Additionally, the efficiency and accuracy of the suggested method estimator in resistance estimation were evaluated using two scenarios.

In the first scenario, Figures 9 and 10 depict the variation of stator and rotor resistance. The resistance values increase linearly up to 100% between 0 and 1 second, then remain constant at twice their nominal value between 1 and 3 (s). Subsequently, the resistance decreases linearly to -50% of its nominal value from 3 to 5 (s) and finally remains constant at -50% of its nominal value after 5 seconds.
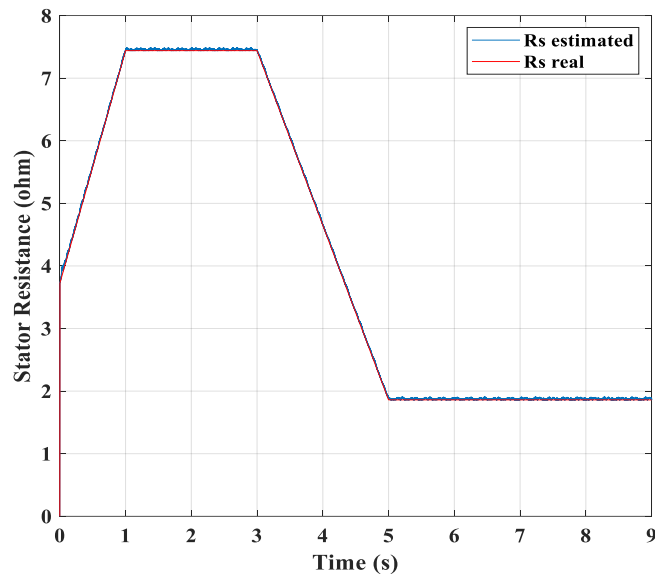
Figure 9. Stator resistance estimation using Fuzzy mutual-MRAS estimator in linear variation
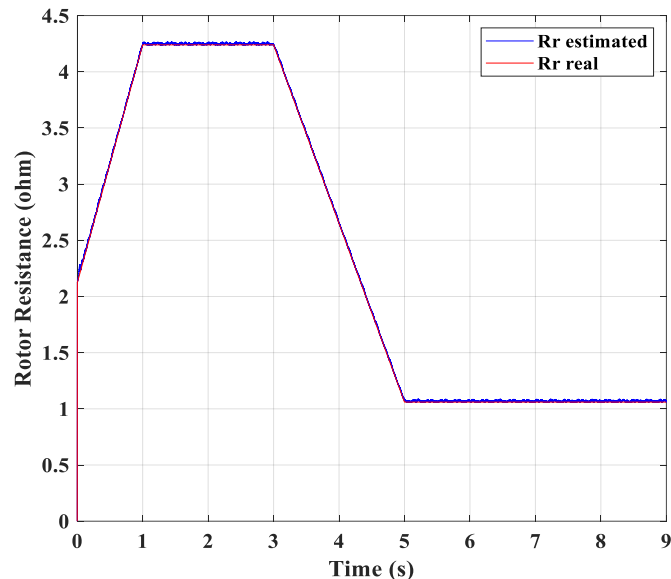
Figure 10. Rotor resistance estimation using Fuzzy mutual-MRAS estimator in linear variation

In the second scenario presented in Figures 11 and 12, the resistance variation is modelled exponentially, which provides a closer representation of real conditions.
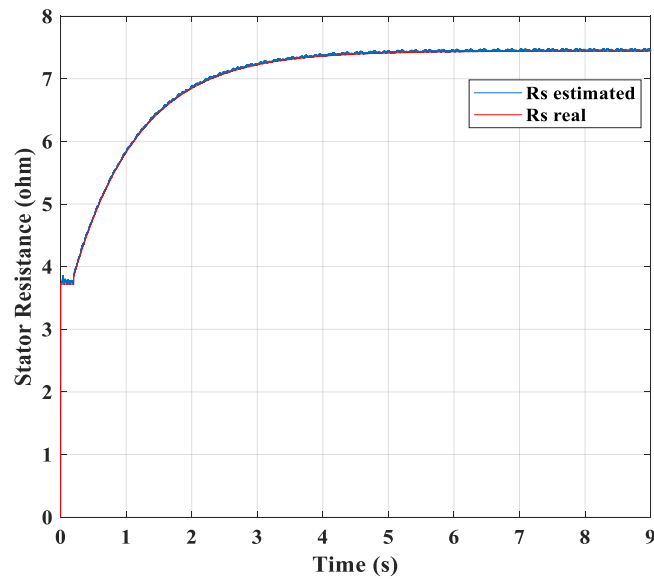
Figure 11. Stator resistance estimation using Fuzzy mutual-MRAS estimator in exponential variation
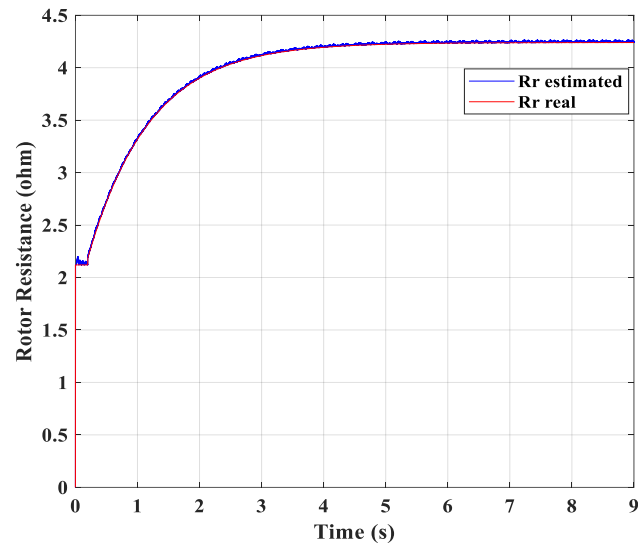
Figure 12. Rotor resistance estimation using Fuzzy mutual-MRAS estimator in exponential variation

From the obtained results depicted in Figures 9 to 12, it is evident that the estimated stator and rotor resistance closely track their real values. Figures 7 and 8 illustrate the decoupling between torque and flux, even in the presence of variable resistance. These findings highlight the effectiveness and robustness of the proposed approach in achieving accurate control and maintaining performance under varying conditions.

6. Conclusion

In this research, the implementation of a parallel fuzzy Mutual-MRAS estimator was utilized to simultaneously estimate the resistances of the stator, rotor, and motor speed. The main objective of this study was to establish a robust sensorless Field-Oriented Control for Dual Star Induction Motors in electric vehicles. The result of the research has effectively accomplished this objective and demonstrated the successful achievement of a reliable and accurate control system for DSIM in electric vehicles. These findings contribute to the advancement of electric vehicle technology and the optimization of motor control systems.

REFERENCES

Andriamalala, R.N., Razik, H. & Sargos, F. M. (November 2008) Indirect-rotor-field-oriented-control of a double-star induction machine using the rst controller. In *2008 34th Annual Conference of IEEE Industrial Electronics*. pp. 3108-3113. IEEE.

Bhatt, P., Mehar, H. & Sahajwani, M. (2019) Electrical motors for electric vehicle–a comparative study. *Proceedings of Recent Advances in Interdisciplinary Trends in Engineering & Applications (RAITEA)*.

Cardenas, R., Pena, R., Proboste, J., Asher, G. & Clare, J. (2005) MRAS observer for sensorless control of standalone doubly fed induction generators. *IEEE Transactions on Energy conversion*. 20(4), 710-718.

Casadei, D., Serra, G., Tani, A., Zarri, L. & Profumo, F. (2003) Performance analysis of a speed-sensorless induction motor drive based on a constant-switching-frequency DTC scheme. *IEEE Transactions on Industry Applications*. 39(2), 476-484.

Chakraborty, C. & Hori, Y. (2003) Fast efficiency optimization techniques for the indirect vector-controlled induction motor drives. *IEEE Transactions on Industry Applications*. 39(4), 1070-1076.

Ehsani, M., Gao, Y., Longo, S. & Ebrahimi, K. M. (2018) *Modern electric, hybrid electric, and fuel cell vehicles*. CRC press.

El Ouanjli, N., Mahfoud, S., Derouich, A., El Daoudi, S. & El Mahfoud, M. (2022) Speed Sensorless Fuzzy Direct Torque Control of Induction Motor Based MRAS Method. *In Digital Technologies and Applications: Proceedings of ICDTA'22, Fez, Morocco, Volume 2*. pp. 779-790. Cham: Springer International Publishing.

Guzinski, J. & Abu-Rub, H. (2012) Speed sensorless induction motor drive with predictive current controller. *IEEE Transactions on Industrial Electronics*. 60(2). pp. 699-709.

Hashemnia, N. & Asaei, B. (September 2008) Comparative study of using different electric motors in the electric vehicles. In *2008 18th International Conference on Electrical Machines*. IEEE. pp. 1-5.

Holmes, D. G., McGrath, B. P. & Parker, S. G. (2011) Current regulation strategies for vector-controlled induction motor drives. *IEEE Transactions on Industrial Electronics*. 59(10). 3680-3689.

Husain, I. & Islam, M. S. (1999) Design, modeling and simulation of an electric vehicle system. *SAE transactions*, 2168-2176.

Jain, J. K., Ghosh, S. & Maity, S. (2020) Concurrent PI controller design for indirect vector controlled induction motor. *Asian Journal of Control*. 22(1), 130-142.

Jin, X., Yin, G. & Chen, N. (2019) Advanced estimation techniques for vehicle system dynamic state: A survey. *Sensors*. 19(19), 4289.

Lian, Y., Zhao, Y., Hu, L. & Tian, Y. (2015) Longitudinal collision avoidance control of electric vehicles based on a new safety distance model and constrained-regenerative-braking-strength-continuity braking force distribution strategy. *IEEE Transactions on Vehicular Technology*. 65(6), pp. 4079-4094.

Merabet, E., Abdessemed, R., Amimeur, H., Hamoudi, F. & Boukhlouf, R.C.M.E.H. (2007) Field-oriented control of a dual star induction machine using fuzzy regulators. *Algorithms*. 6, 12.

Mitronikas, E. D., Safacas, A. N. & Tatakis, E. C. (2001) A new stator resistance tuning method for stator-flux-oriented vector-controlled induction motor drive. *IEEE Transactions on Industrial Electronics*. 48(6), 1148-1157.

Montanari, M., Peresada, S. M., Rossi, C. & Tilli, A. (2007) Speed sensorless control of induction motors based on a reduced-order adaptive observer. *IEEE Transactions on Control Systems Technology*. 15(6), 1049-1064.

Pellegrino, G., Vagati, A., Guglielmi, P. & Boazzo, B. (2011) Performance comparison between surface-mounted and interior PM motor drives for electric vehicle application. *IEEE Transactions on Industrial Electronics.* 59(2), 803-811.

Rsn, R., Rs, R., Ls, L., Cr, C. & Kf, J. (2016) Performances des structures mutuelles adaptatives MRAS et MRAS-Flou appliquées au contrôle sans capteur de vitesse pour actionneurs asynchrones. *Communication Science &technology*. 16, 12-22.

Sadouni, R. and Meroufel, A., 2012. Indirect rotor field-oriented control (IRFOC) of a dual star induction machine (DSIM) using a fuzzy controller. *Acta Polytechnica Hungarica*. 9(4), 177-192.

Sahraoui, K., Ameur, A. & Kouzi, K. (November 2018) Performance enhancement of sensorless speed control of DSIM using MRAS and EKF optimized by genetic algorithm. In *2018 International Conference on Applied Smart Systems (ICASS).* IEEE. pp. 1-8.

Sahraoui, K., Kouzi, K. & Ameur, A. (2017) Optimization of MRAS based Speed Estimation for Speed Sensorless Control of DSIM via Genetic Algorithm. *Electrotehnica, Electronica, Automatica*. 65(3), 156-162.

Singh, R. Kachhwaha, M. & Fulwani, D. M. (2022) MRAS-based Integral Sliding Mode Control of Electric Vehicles under Speed and Load Torque Fluctuations. *IEEE International Conference on Power Electronics, Drives and Energy Systems (PEDES), Jaipur, Indi.* pp. 1-6.

Touam, M., Chenafa, M. & Chekroun, S. (2021) Sensorless nonlinear sliding mode control of the induction machine at very low speed using FM-MRAS observer. *International Journal of Power Electronics and Drive Systems.* 12(4), 1987.

Verma, V., Chakraborty, C., Maiti, S. & Hori, Y. (2013) Speed sensorless vector controlled induction motor drive using single current sensor. *IEEE Transactions on Energy Conversion*. 28(4), 938-950.

Yang, G. & Chin, T. H. (1993) Adaptive-speed identification scheme for a vector-controlled speed sensorless inverter-induction motor drive. *IEEE Transactions on Industry Applications*. 29(4), 820-825.

Ismail BENMILOUD was born in Laghouat, Algeria, in 1996. He received his M.Sc. from Amar Telidji University of Laghouat in 2020. Currently, he is a Ph.D. student at the same University. His current research interests include Advanced control of Electric vehicles and power converters.

Katia KOUZI was born in Algeria. She obtained her Engineer and Master's Degrees in Electrical Engineering in 1998 and 2002. She received her Ph.D. degree in Electrical and Computer Engineering from the University of Batna, in 2008. Her research interests are focused on the Advanced Control of AC Drives, including Vector, Sensorless, Intelligent Artificial Control, Electric vehicles (EVs) control, Renewable Energy Systems Control, Managements and Storage Systems. She is a researcher in the Semiconductors and Functional Materials Laboratory, as well as a full professor at the Electrical Engineering Institute at Laghouat University, Algeria.

Aissa AMEUR was born in Laghouat, Algeria, in 1971. He obtained his Magister and Ph.D. degrees in Electrical Engineering in 2005 and 2012, from Batna University, Algeria. In 2005, he joined the Electrical Engineering Department of Laghouat University, Algeria as Assistant Lecturer. Since May 2012, Dr Ameur is an Assistant Professor in the same department. He is a researcher in the LeDMaScD laboratory, at Laghouat University, Algeria. His main research interests include Modelling of Electrical Machines, Electrical Drives Control, Fault Diagnosis, Artificial Intelligence and Renewable Energy Systems Control.